THE JOURNAL OF BIOLOGICAL CHEMISTRY
Vol. 277, No. 52, Issue of December 27, pp. 50365–50372, 2002
Printed in U.S.A.

Ca^{2+}-Myristoyl Switch in the Neuronal Calcium Sensor Recoverin Requires Different Functions of Ca^{2+}-binding Sites*

Received for publication, May 3, 2002, and in revised form, September 26, 2002
Published, JBC Papers in Press, October 21, 2002, DOI 10.1074/jbc.M204338200

Ivan I. Senin‡, Torsten Fischer§, Konstantin E. Komolov‡, Dimitry V. Zinchenko¶, Pavel P. Philippov‡ and Karl-Wilhelm Koch§‖

From the ‡A. N. Belozersky Institute of Physico-Chemical Biology, Moscow State University, 119992 Moscow, Russia, §Institut für Biologische Informationsverarbeitung 1, Forschungszentrum Jülich, D-52425 Jülich, Germany, and ¶Branch of Shemyakin and Ovchinnikov Institute of Bioorganic Chemistry, Puschino, 142292 Moscow, Russia

Recoverin is an EF-hand Ca^{2+}-binding protein that is suggested to control the activity of the G-protein-coupled receptor kinase GRK-1 or rhodopsin kinase in a Ca^{2+}-dependent manner. It undergoes a Ca^{2+}-myristoyl switch when Ca^{2+} binds to EF-hand 2 and 3. We investigated the mechanism of this switch by the use of point mutations in EF-hand 2 (E85Q) and 3 (E121Q) that impair their Ca^{2+} binding. EF-hand 2 and 3 display different properties and serve different functions. Binding of Ca^{2+} to recoverin is a sequential process, wherein EF-hand 3 is occupied first followed by the filling of EF-hand 2. After EF-hand 3 bound Ca^{2+}, the subsequent filling of EF-hand 2 triggers the exposition of the myristoyl group and in turn binding of recoverin to membranes. In addition, EF-hand 2 controls the mean residence time of recoverin at membranes by decreasing the dissociation rate of recoverin from membranes by 10-fold. We discuss this mechanism as one critical step for inhibition of rhodopsin kinase by recoverin.

G-protein-coupled receptor kinases provide desensitization of G-protein-coupled receptors by phosphorylation of serine and threonine residues at their cytoplasmic C terminus (1). A well-known system represents the light absorbing pigment rhodopsin and the corresponding kinase, rhodopsin kinase, or GRK-1, which phosphorylates (and thus desensitizes) photobleached rhodopsin. Arrestin then binds to phosphorylated rhodopsin and thereby stops any further activation of the G-protein transducin (2, 3). Illumination causes the decrease in the concentration of the intracellular transmitters of excitation and adaption, cGMP and cytoplasmic [Ca^{2+}], respectively. The decrease in cytoplasmic [Ca^{2+}] is sensed by Ca^{2+} sensor proteins such as recoverin (4–6; for a recent review, see Ref. 7). Recoverin or the amphibian orthologue S-modulin (8, 9) inhibit rhodopsin kinase at high levels of free [Ca^{2+}], thereby relieving inhibition when the Ca^{2+} level decreases. The Ca^{2+}-dependent control of rhodopsin kinase via recoverin belongs to at least nine different mechanisms in vertebrate photoreceptor cells that control adaptation to background light intensities (10–13).

Of particular importance for recoverin as a Ca^{2+} sensor of rhodopsin kinase is its Ca^{2+}-myristoyl switch (14, 15). A combination of biochemical and structural ^{1}H-NMR approaches has deciphered some of the molecular details of this switch mechanism; recoverin has a compact structure and consists of two domains. Each domain harbors two EF-hand structures but only EF-hand 2 and 3 can bind Ca^{2+} ions. Retinal recoverin is heterogeneously acylated (mainly myristoylated) at its N terminus (16). The myristoyl group is sequestered within a hydrophobic pocket when no Ca^{2+} ions are bound to recoverin. Extrusion of the myristoyl group is triggered by binding of Ca^{2+}, which then enables recoverin to associate with phospholipid membranes (17–19).

Myristoyl switches are not restricted to recoverin and its homologue neuronal calcium sensor proteins (reviewed in 20–22); instead, myristoyl switches are also found in other signal transduction proteins. For example, a Ca^{2+}-myristoyl/palmitoyl switch mechanism operates in the protozoan *Trypanosoma cruzi* and translocates a 24-kDa Ca^{2+}-binding protein to the flagellar membrane (23). Another type of myristoyl switch works in ADP-ribosylation factors, which control the assembly and disassembly of transport vesicle coats. These small GTP-binding proteins undergo GDP/GTP-exchange, which triggers the exposure of the myristoyl group (24, 25). A phosphorylation-dependent myristoyl switch is present in myristoylated alanine-rich C kinase substrates and Src kinases, where phosphorylation triggers the release of these proteins from the membrane (26). Thus, myristoyl switches operate in a wide range of signaling systems, but they share common themes in their mechanisms: a trigger such as Ca^{2+} ions, GDP/GTP exchange, or phosphorylation induces exposition of the fatty acyl group and consequently translocation of the protein.

To understand the mechanism of the Ca^{2+}-myristoyl switch in greater molecular detail, we used recoverin mutants with impaired EF-hand Ca^{2+}-binding sites (27). For this purpose, we introduced the substitutions E85Q (mutant Rc^{E85Q}) and E121Q (mutant Rc^{E121Q}) in EF-hand 2 and EF-hand 3 of recoverin, respectively, because we know that substitutions in the Z position of the loop of the EF-hand motif decrease the affinity of the Ca^{2+}-binding site for Ca^{2+} by about 1000-fold (28, 29). The structure of myristoylated Rc^{E85Q} with one Ca^{2+} ion bound was recently published and represents an intermediate state between the structures of recoverin with zero and two Ca^{2+} ions bound (30). The myristoyl group in Rc^{E85Q} is partially buried, and it was predicted that the mutant RcE85Q would not exhibit any considerable binding to membranes (30). The importance of the positions Glu-85 and Glu-121 was also described for S-modulin in a study by Matsuda *et al.* (31). These authors reported on sequential Ca^{2+} binding and showed that

* This work was supported by grants from the Deutsche Forschungsgemeinschaft (to K.-W. K), a grant from the Forschungszentrum Jülich for visiting scientists (to I. I. S., K. E. K., and P. P. P.), the Ludwig Institute for Cancer Research (to P. P. P.), "International Projects" of Ministry of Industry and Science, Russian Federation (to P. P. P.), and Russian Foundation for Basic Research Grants 00-04-48332 (to P. P. P.), 00-04-48332 (to I. I. S.), and 00-04-48332 (to K. E. K.). The costs of publication of this article were defrayed in part by the payment of page charges. This article must therefore be hereby marked "*advertisement*" in accordance with 18 U.S.C. Section 1734 solely to indicate this fact.

‖ To whom correspondence should be addressed. Tel.: 49-2461-61-3255; Fax: 49-2461-614216; E-mail: k.w.koch@fz-juelich.de.

the S-modulin mutant E85M bound only one Ca^{2+}, but it associated with membranes similar to the wild type. These data were in contrast to the prediction based on the three-dimensional structure of Rc^{E85Q}. We used the recoverin mutants Rc^{E85Q} and Rc^{E121Q} to study the Ca^{2+}-myristoyl switch in more detail and measured binding of WT[1]-recoverin and the mutants to rod outer segment (ROS) membranes and liposomes; in particular, we studied the dynamics of the binding to liposomes by surface plasmon resonance (SPR) spectroscopy.

EXPERIMENTAL PROCEDURES

Materials—$^{45}CaCl_2$ was purchased from Amersham Biosciences. All other chemicals were obtained from Merck, Sigma, Amersham Biosciences, and Fluka. Bovine brain phosphatidylcholine, bovine brain phosphatidylserine and egg yolk phosphatidylethanolamine were from Sigma and 98% pure. Polycarbonate filter membranes (type GTTP) were from Millipore. All other reagents and buffers were at least analytical grade.

Preparation of ROS—Bovine ROS were prepared from fresh bovine retinae and stored at −80 °C as described previously (32). Urea-washed ROS membranes were obtained by the homogenization of ROS in 5 M urea and 20 mM Tris-HCl, pH 7.5, in the dark (33). Then ROS were incubated on ice for 5 min and were centrifuged at 100,000 × *g* for 40 min at 4 °C. The pellet was resuspended and washed three times with buffer (20 mM Tris-HCl, pH 7.5, 2 mM $MgCl_2$, 0.1 mM EDTA, 1 mM DTT, and 1 mM phenylmethylsulfonyl fluoride) and stored at −80 °C.

Preparation of Recoverin and Recoverin Mutants—Mutagenesis of recoverin was described previously (27). Recombinant nonmyristoylated and myristoylated forms of recoverin and its mutants were expressed in the *E. coli* strains pET11d rec/BL21 and pET11d rec/pBB131/BL21C, respectively. Cells were lysed in buffer B (20 mM Tris-HCl, pH 8.0, 100 mM NaCl, 1 mM DTT, 1 mM phenylmethylsulfonyl fluoride, 0.1 mM EDTA, 0.2 mM EGTA) including 0.05 mg/ml lysozyme, incubated on ice for 20 min and centrifuged at 15000g for 20 min at 4 °C. The supernatant was adjusted to 2 mM or 20 mM $CaCl_2$ for WT-recoverin and Rc^{E121Q}, respectively, and was applied to a phenyl-Sepharose column previously equilibrated with buffer B containing 2 mM or 20 mM $CaCl_2$. Recoverin was eluted with buffer B containing 2 mM EGTA. In the case of mutant Rc^{E85Q}, a gel filtration on a Superose 12 (AmershamPhamacia Biotech) was used instead of chromatography on a phenyl-Sepharose. The fraction containing recoverin was loaded on a Mono-Q (5/5) column that was equilibrated with 20 mM Tris-HCl, pH 8.0, 1 mM DTT, and 1 mM phenylmethylsulfonyl fluoride. Nonmyristoylated and myristoylated recoverin were eluted with a linear gradient of 0–400 mM NaCl in 20 mM Tris-HCl, pH 8.0. The purity of recoverin was evaluated by SDS-polyacrylamide gel electrophoresis with Coomassie Brilliant Blue staining.

The degree of myristoylation was determined by analytical high performance liquid chromatography and was, in most cases, more than 95%. Only WT recoverin showed a lower degree of myristoylation (70–80%) and was purified to a homogeneous myristoylated form by high performance liquid chromatography. Denatured protein was refolded as described in Ref. 34.

$^{45}Ca^{2+}$-binding Assay—All buffers and protein solutions used in Ca^{2+} titration experiments were passed over a Chelex column (Bio-Rad) to remove residual amounts of Ca^{2+}. Chelex resin was prepared and equilibrated according to the manufacturer's instructions. Binding of $^{45}Ca^{2+}$ was performed as described previously (17). Briefly, samples (0.5 ml) that contained 50 or 100 μM protein were dissolved in 20 mM HEPES, pH 7.5, 100 mM NaCl, and 1 mM DTT and were transferred to Centricon 10 devices (Amicon). A solution of 10 μl of 0.2 mM $^{45}CaCl_2$ (0.4–0.5 μCi) solution was added and centrifuged for 1 min at 30 °C (7000 rpm) in a tabletop centrifuge (model TJ-6; Beckman Coulter). After centrifugation, the radioactivity in 15 μl of the filtrate (free Ca^{2+}) and an equal volume of protein sample (total Ca^{2+}) were determined by liquid scintillation counting. On the next steps, nonradioactive $CaCl_2$ was added and the centrifugation procedure above was repeated. Protein-bound Ca^{2+} *versus* free Ca^{2+} was determined from the excess Ca^{2+} in the protein sample over that present in the ultrafiltrate. The data were analyzed as follows: $Ca^{2+}{}_{free} = R_f/R_p \times Ca^{2+}{}_{total}$, where R_f is the radioactivity in the filtrate, R_p is radioactivity in protein sample, and $Ca^{2+}{}_{total}$ and $Ca^{2+}{}_{free}$ are the total and free Ca^{2+} concentration, respectively.

Preparation of Ca^{2+} Buffer and Determination of Free Ca^{2+} Concentration—Free Ca^{2+}concentrations of buffer solutions were calculated using the program Webmax 2.0 (Stanford University). We used dibromo-BAPTA as Ca^{2+} buffer in Ca^{2+} titration experiments (35). The free Ca^{2+} concentration of buffer solutions was checked with a Ca^{2+}-sensitive electrode (World Precision Instruments, Inc.) using calibration standards in the range from 10^{-8} to 10^{-1} M free $[Ca^{2+}]$.

Equilibrium Centrifugation Assay—Binding of recoverin to ROS membranes was performed according to a published procedure (14). Briefly, 30 μM recoverin or its mutants were mixed with bleached, urea-washed ROS membranes (50 μM rhodopsin) and incubated at 37 °C (Eppendorf Thermomixer 5436, 1000 rpm) for 15 min in 20 mM HEPES, pH 7.5, 150 mM NaCl, 20 mM $MgCl_2$, 1 mM DTT, 3 mM dibromo-BAPTA, and 0–50 mM $CaCl_2$ (total volume 75 μl). Membranes were separated by centrifugation (15 min, 14,000 rpm; Eppendorf model 5415 tabletop centrifuge) and the supernatant was removed. The pellet was analyzed by SDS-PAGE.

Protein Concentration and Electrophoresis—Protein concentrations were determined by a Bradford assay (36) using a recoverin calibration curve. SDS-PAGE was performed as described previously (37).

Preparation of Liposomes—Liposomes were prepared as described previously (38) with slight modification. A mixture of 4 mg of lipids (40% (w/w) phosphatidylethanolamine, 40% (w/w) phosphatidylcholine, 15% (w/w) phosphatidylserine; 5% (w/w) cholesterol corresponding to the lipid composition in bovine ROS membranes in $CHCl_3$ was dried down by vacuum in a SpeedVac concentrator. The sample was resuspended in 2 ml of degassed buffer (20 mM HEPES, pH 7.5, 150 mM KCl, and 3 mM EGTA) and sonified for 2 × 15 min (Branson B12; cup; 100 W). Large unilamellar vesicles (liposomes) were produced using the extrusion technique. The suspension was soaked for 15–20 min and extruded through polycarbonate filter with a pore diameter of 1 μm (first step) and 0.4 μm (second step).

Surface Plasmon Resonance Measurements and Data Evaluation—Binding of recoverin to liposomes and ROS membranes was monitored by surface plasmon resonance (BIAcore) as described previously (38). The running buffer contained 10 mM HEPES, pH 7.5, 150 mM KCl, 20 mM $MgCl_2$, and Ca^{2+} buffers as indicated. Liposomes were immobilized on a sensor chip with a self-assembled monolayer of alkanethiols or, alternatively, by binding on a hydrophobic sensor chip (pioneer L1; BIAcore). Nonspecific binding was tested by application of bovine serum albumin. Interaction of recoverin with immobilized liposomes or ROS vesicles was tested by applying 2–75 μM protein in running buffer at different $[Ca^{2+}]$. Free $[Ca^{2+}]$ was adjusted with dibromo-BAPTA as Ca^{2+} buffer. The flow rate was 5 μl/min. Resonance signals at equilibrium were determined and normalized to the amount of immobilized phospholipids that allows the direct comparison of recordings obtained with different surfaces. Data evaluation was performed with the software BIAevaluation 3.1. Sensorgrams were evaluated by nonlinear curve fitting according to a model of two parallel reactions. Using this procedure, we determined relative kinetics of a fast and slow component in the dissociation phase. The Ca^{2+}-dependent development of the slower component in the dissociation phase was analyzed by comparing the relative response at 10 s after start of the dissociation process. The amplitude of each sensorgram at that time was determined and was assigned RU_t. The maximal amplitude of the corresponding sensorgram was RU_{max}.

RESULTS

Ca^{2+}-dependent Binding of Myristoylated WT-Recoverin and Recoverin Mutants to Rod Outer Segment Membranes—We first tested the binding of $^{45}Ca^{2+}$ to myristoylated forms of WT-recoverin and mutants Rc^{E85Q} and Rc^{E121Q}, which were obtained as homogeneous protein preparations. At saturating Ca^{2+} concentrations (above 100 μM), WT-recoverin bound two Ca^{2+}, Rc^{E85Q} bound 1.1 Ca^{2+} and Rc^{E121Q} did not bind Ca^{2+} (Fig. 1). Binding of Ca^{2+} to WT-recoverin was half-maximal at 17.6 μM (Hill coefficient, $n_H = 1.9$). Ca^{2+}-binding data for Rc^{E85Q} reached a plateau (*i.e.* apparently saturated) above 100 μM; however, when we increased the Ca^{2+} concentration to 2–10 mM, an additional increase in Ca^{2+} binding was observed (Fig. 1). We interpret the last finding to indicate binding of Ca^{2+} to the mutated second EF-hand with low affinity. Binding of Ca^{2+} to Rc^{E85Q} was half-maximal at 34.6 μM (Hill coefficient, $n_H = 1.0$).

[1] The abbreviations used are: WT, wild type; ROS, rod outer segment; DTT, dithiothreitol; BAPTA, 1,2-bis(2-aminophenoxy)ethane-*N*,*N*,*N*′,*N*′-tetraacetic acid; RU, resonance units; SPR, surface plasmon resonance.

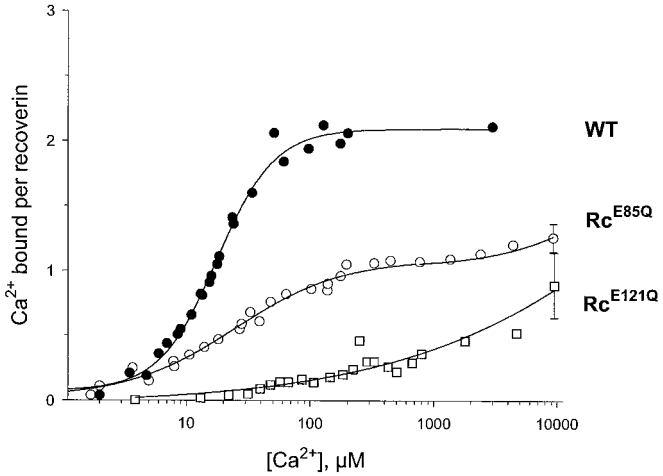

FIG. 1. **$^{45}Ca^{2+}$ binding to recoverin and recoverin mutants.** Myristoylated WT-recoverin (●), Rc^{E85Q} (○), and Rc^{E121Q} (□) were incubated with increasing free $[Ca^{2+}]$. *Solid lines* represent the best fit to the Hill model (myristoylated WT-recoverin, K_D = 17.6 μM, n = 1.9; myristoylated Rc^{E85Q}, K_D = 34.6 μM and n = 1.0).

Our results on Ca^{2+} binding to WT-recoverin were in agreement with previous work (17). The binding experiments with the mutants showed that impairment of the second EF-hand leads to binding of one Ca^{2+}, whereas impairment of the third EF-hand prevents binding of Ca^{2+} to both sites. Initial characterization of the mutants had proven that their general structure had not changed (39). Thus, mutants Rc^{E85Q} and Rc^{E121Q} can serve as selective tools to study the Ca^{2+}-myristoyl switch.

One approach to study the Ca^{2+}-myristoyl switch of recoverin is to determine the amount of membrane-associated recoverin under varying Ca^{2+} concentrations. Myristoylated forms of WT-recoverin and the mutants were incubated with washed ROS membranes at different free $[Ca^{2+}]$ from 117 nM to 50 mM. Non-bound recoverin was removed by centrifugation, and the amount of bound recoverin was determined by densitometric scanning of Coomassie Blue-stained gels.

A representative example is displayed in Fig. 2*A* for WT-recoverin and mutants Rc^{E85Q} and Rc^{E121Q}. The relative intensity of recoverin bands is shown as a function of free $[Ca^{2+}]$ in Fig. 2*B*. Half-maximal binding of WT-recoverin and Rc^{E121Q} to ROS membranes was at 4.7 μM and 5 mM, respectively. The binding of Rc^{E121Q} to ROS membranes with an EC_{50} of 5 mM Ca^{2+} (Fig. 2*B*) is far beyond the working range of the Ca^{2+}-myristoyl switch in WT-recoverin and might reflect the low-affinity binding of Ca^{2+} to the mutated EF-hand 3 (39), which allows Ca^{2+} to fill the native EF-hand 2 and to trigger binding of the mutant to the membranes. A special observation was made with Rc^{E85Q}. Binding of this mutant to ROS membranes occurred in two steps, reaching a first plateau around 100 μM and full saturation above 10 mM (Fig. 2*B*). The data profile was reminiscent of $^{45}Ca^{2+}$ binding to nonmyristoylated recoverin (*i.e.* binding to two independent sites; see Fig. 2*A* in Ref. 17). Therefore, the data were well-fit according to a model of two independent binding sites yielding two EC_{50} values of half-maximal binding of Rc^{E85Q} to ROS membranes equal to 9 μM and 2.6 mM.

Binding of Myristoylated WT-Recoverin to Liposomes Immobilized on a Sensor Chip—In a second approach to studying the Ca^{2+}-myristoyl switch of recoverin, we applied SPR spectroscopy to record binding of myristoylated WT-recoverin and mutants Rc^{E85Q} and Rc^{E121Q} to phospolipid liposomes. SPR spectroscopy allows the quantification of the affinity of a binding reaction and, in addition, can provide insight into the kinetics of a binding reaction.

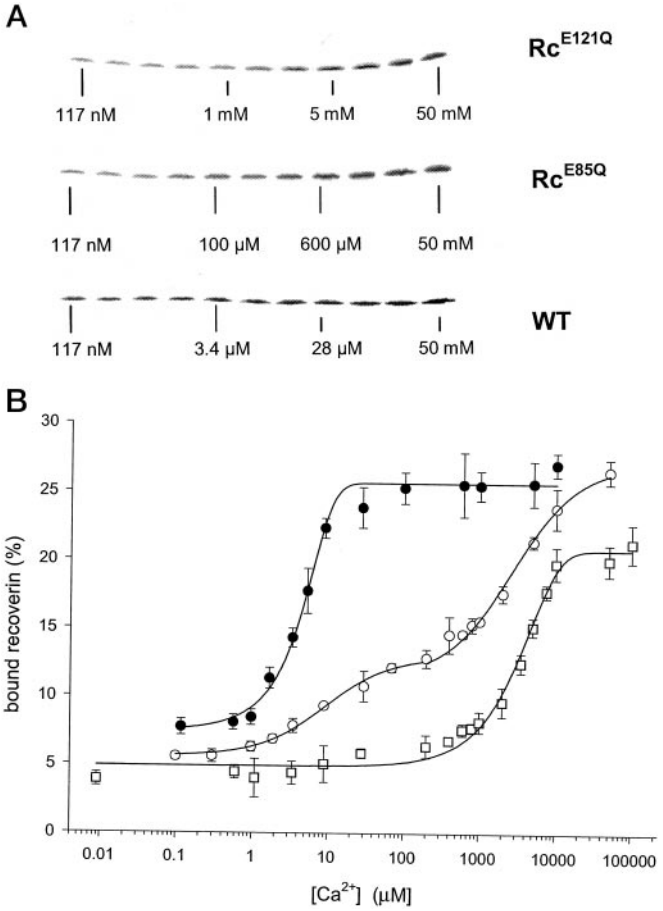

FIG. 2. **Ca^{2+}-dependent binding of WT-recoverin and recoverin mutants to ROS membranes.** *A*, Coomassie Blue stained SDS-polyacrylamide gels showing the presence of Rc^{E121Q} (*top trace*), Rc^{E85Q} (*middle trace*), and WT-recoverin (*bottom trace*) at ROS membranes after centrifugation. The free $[Ca^{2+}]$ is shown below the corresponding protein bands for a few selected bands. The complete ranges are 117 nM, 570 nM, 200 μM, 600 μM, 1 mM, 2 mM, 3.5 mM, 5 mM, 7.5 mM, 10 mM, and 50 mM for Rc^{E121Q}; 117 nM, 3.4 μM, 5.3 μM, 9 μM, 100 μM, 200 μM, 400 μM, 600 μM, 800 μM, 10 mM, and 50 mM for Rc^{E85Q}; and 117 nM, 570 nM, 980 nM, 1.7 μM, 3.4 μM, 5.3 μM, 9 μM, 28 μM, 100 μM, 1 mM, and 50 mM for WT-recoverin. *B*, quantitative determination of bound WT-recoverin (●), Rc^{E85Q} (○), and Rc^{E121Q} (□) to ROS membranes by densitometric scanning of Coomassie Brilliant Blue-stained gels as shown in A, yielding an EC_{50} = 4.7 μM and n = 1.8 for WT-recoverin, EC^1_{50} = 9 μM and EC^2_{50} = 2.6 mM for Rc^{E85Q}, and EC_{50} = 3 mM, n = 1.6 for Rc^{E121Q}. Data points are from two to six different evaluations.

We immobilized phospholipid liposomes using a hydrophobic sensor chip (pioneer L1; BIAcore) to capture phospholipids that were injected over the flow cell. Immobilized liposomes were stable over the time course of a typical experiment and could be used to monitor association and dissociation of recoverin by SPR-spectroscopy.

First, we tested whether the system was suitable for our application. When myristoylated WT-recoverin was supplied in the mobile phase, binding of recoverin to immobilized liposomes on the sensor chip caused a change in resonance units (RU) and was recorded as a sensorgram (Fig. 3*A*). The *black bar* in Fig. 3*A* indicates the association phase of the sensorgram. The association phase attained a plateau during injection of recoverin, which indicates that the binding of recoverin to liposomes had reached equilibrium. Dissociation of recoverin from liposomes was triggered by flushing the flow cell with running buffer without recoverin (Fig. 3, *open bar*). Complete dissociation of recoverin from liposomes was achieved by a short pulse of 10 mM Ca^{2+} chelator EGTA during the dissociation phase (not shown). Sensorgrams were recorded at differ-

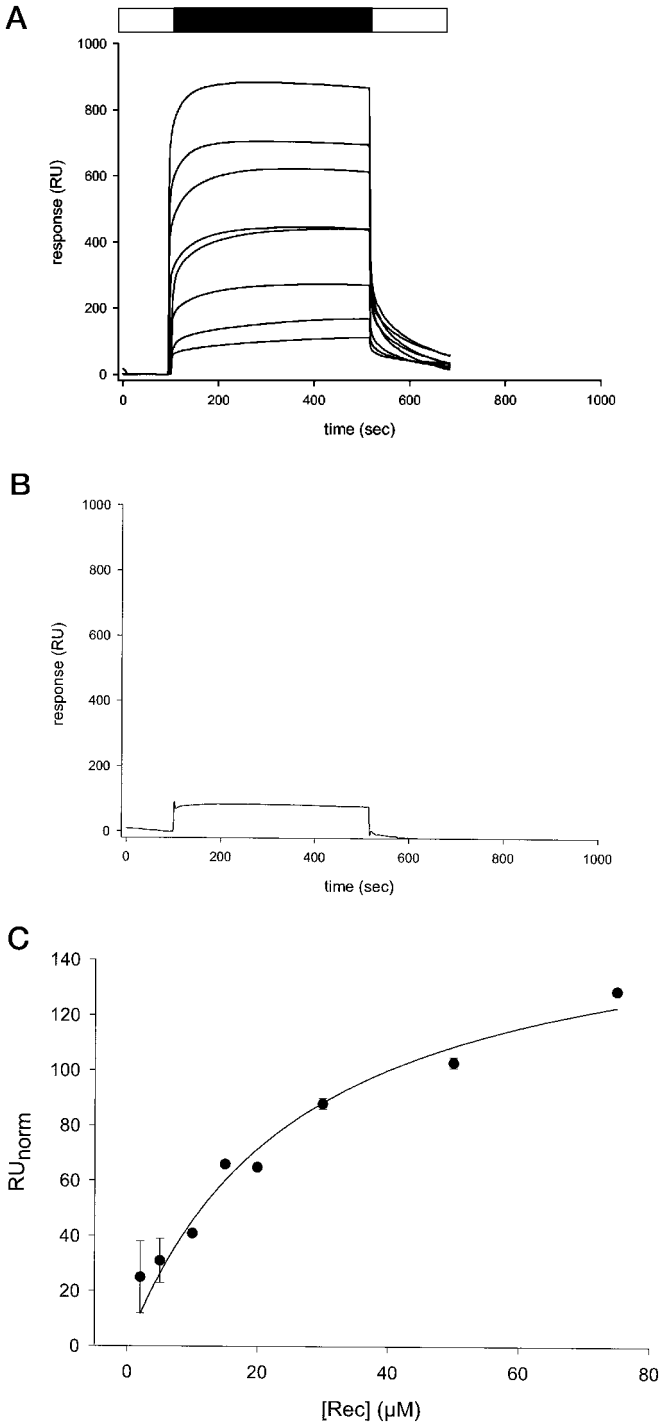

FIG. 3. **Quantitative analysis of WT-recoverin binding to immobilized liposomes by SPR spectroscopy.** *A*, a representative overlay of sensorgrams recorded with different concentrations of myristoylated WT-recoverin is displayed. WT-recoverin at 2, 4, 5, 10, 15, 20, 30, 50, and 75 μM was injected into the running buffer and association (*black bar*) to immobilized liposomes was recorded. *B*, control recording with 30 μM protein G. *C*, maximal resonance signals at equilibrium were determined, normalized, and are shown as a function of the WT-recoverin concentration. Data are from two sets of recordings; EC_{50} = 26 μM.

ent concentrations of recoverin (Fig. 3*A*). At all concentrations used, sensorgrams showed rapid association and dissociation of recoverin. Thus, myristoylated recoverin did not permanently stay on the membrane; instead, there was a rapid equilibrium between the bound and soluble states.

Because a bulk refractive index change could lead to an increase in RU without reflecting any true binding to immobilized liposomes, we performed three control experiments to exclude this possibility. 1) We applied 30 μM calmodulin or protein G to measure the change in bulk refractive index that might be caused by a protein solution of comparable concentration (Fig. 3*B*). Injection of calmodulin and protein G both caused a change of 70–80 RU or 8.5–9.8 RU_{norm} (normalized to the amount of immmobilized lipids). 2) When we used a running buffer that contained the Ca^{2+} chelator EGTA instead of Ca^{2+}, we observed signals with amplitude between 67 and 89 RU (data not shown). Amplitudes did not differ much when we used either WT-recoverin or recoverin mutants in EGTA buffer. 3) When nonmyristoylated WT-recoverin was injected, the recorded change was 107–115 RU and 116–125 RU in the presence and absence of Ca^{2+}, respectively. Thus, nonmyristoylated WT-recoverin did not undergo a specific Ca^{2+}-dependent binding to membranes, which is consistent with previous observations (14, 38). Together, these control recordings showed that a change in bulk refractive index of a protein solution is similar to the signal obtained with myristoylated recoverin forms in the absence of Ca^{2+}. Thus, a Ca^{2+}-dependent change in RU, which is below 70–80 RU, reflects unspecific binding to immobilized lipids.

Half-maximal binding of myristoylated WT-recoverin to immobilized lipids was determined from a plot of the normalized amplitude at equilibrium (RU_{norm}) as a function of the recoverin concentration (Fig. 3*C*). We estimated an EC_{50} of 26 μM for myristoylated WT-recoverin, which is similar to the value obtained by Lange and Koch (38) with ROS liposomes and a different immobilization strategy. Therefore, our experiments showed that 1) a Ca^{2+}-dependent association of recoverin with membranes can be recorded on a sensor chip surface with immobilized liposomes, 2) the association is reversible, and 3) the binding proceeds in a recoverin concentration-dependent manner with moderate affinity. These experimental observations therefore reflect the Ca^{2+}-myristoyl switch of recoverin.

Binding of Myristoylated Recoverin Mutants to Liposomes Recorded by SPR Spectroscopy—We next tested by SPR spectroscopy whether myristoylated recoverin mutants bind to liposomes immobilized on a sensor chip surface by the same protocols as described above for WT-recoverin. First, binding was tested at 100 μM Ca^{2+}, 1 mM Ca^{2+}, and no Ca^{2+} present and second, in the case of binding, the apparent affinity of mutants for membranes was determined. Myristoylated mutant Rc^{E121Q} showed small signals of the same amplitude at 100 μM Ca^{2+}, 1 mM Ca^{2+}, and 0 Ca^{2+} (data not shown). In the presence of 2 mM Ca^{2+}, injection of Rc^{E121Q} elicited a response of ~80 RU. Because this maximal amplitude was identical to changes in RU obtained in control recordings, we conclude that Rc^{E121Q} does not show a Ca^{2+}-myristoyl switch in the range of free Ca^{2+} from 0 to 2 mM. It was impossible to monitor Ca^{2+}-dependent binding of Rc^{E121Q} to immobilized liposomes by SPR spectroscopy at higher Ca^{2+} concentrations like it was tested in the equilibrium centrifugation assay (above). We observed in several independent experiments that recordings at high [Ca^{2+}] (≥1–2 mM) were less accurate than when we used lower concentrations of Ca^{2+}. Amplitudes increased because of some nonspecific matrix effects.

Myristoylated mutant Rc^{E85Q} exhibited properties different from those of Rc^{E121Q}: binding amplitudes at 100 μM Ca^{2+} were higher than in the absence of Ca^{2+}, and the amplitude further increased when Ca^{2+} was 1 mM (for example, see Figs. 4 and 5*A*). The amplitudes (240–250 RU) were also significantly higher than control recordings with calmodulin or protein G (Fig. 3*B*). Thus, we conclude that in mutant Rc^{E85Q}, in contrast to Rc^{E121Q}, the Ca^{2+}-myristoyl switch is operative.

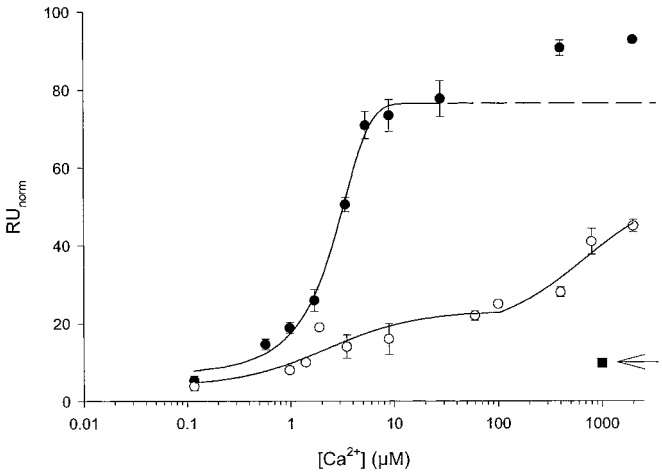

FIG. 4. **Ca^{2+} titration of recoverin-liposome interaction.** Binding of myristoylated WT recoverin (●) and myristoylated Rc^{E85Q} (○) to liposomes was measured at different free [Ca^{2+}] by SPR spectroscopy. Maximal amplitudes of resonance signals at equilibrium were determined and normalized (Fig. 3). Normalized RU values are shown as a function of free [Ca^{2+}]. Values at 1 and 2 mM Ca^{2+} were slightly above the calculated curve because of some additional nonspecific matrix effects. The *arrow* points to the value obtained in the control recordings with calmodulin and protein G.

Binding of Myristoylated Forms of WT-Recoverin and Mutant Rc^{E85Q} to Liposomes as a Function of Ca^{2+} Concentration—A critical parameter of the Ca^{2+}-myristoyl switch is the free [Ca^{2+}] at which the effect is half-maximal. Therefore, we determined the free [Ca^{2+}] at which binding of myristoylated forms of WT-recoverin and mutant Rc^{E85Q} to immmobilized liposomes is half-maximal (Fig. 4). The mutant Rc^{E121Q} was not further considered, because it did not show any Ca^{2+}-dependent binding to membranes within the range of 0.1 μM to 2 mM. Binding of WT-recoverin as a function of [Ca^{2+}] showed a sigmoidal dependence with an EC_{50} of 2.2 μM and a Hill coefficient of 1.4. In contrast, binding of Rc^{E85Q} to membranes differed in several aspects: the maximal amplitude at 1 and 2 mM Ca^{2+} was less than half of the value observed with the WT-recoverin, a first plateau of binding was visible around 100 μM Ca^{2+}, and at higher Ca^{2+} concentrations, the data points did not reach a clear saturation. We did not extend the titration to higher Ca^{2+} concentrations, because nonspecific matrix effects of the sensor chip became prominent (see also above). The *arrow* in Fig. 4 points to the value obtained from a control measurement with protein G at 1 mM Ca^{2+}. Amplitudes of these control measurements include nonspecific binding as well as nonspecific matrix effects. We can roughly calculate that any nonspecific matrix effect at 1 mM Ca^{2+} would constitute less than 10% of the amplitude obtained with WT-recoverin and Rc^{E85Q}.

Data in Fig. 4 seemed similar to data in Fig. 2*B* for Rc^{E85Q} binding to ROS membranes (note plateau around 100 μM Ca^{2+}) and thus could be fit by a model of two independent binding sites (see above and Ref. 17). In so doing, we obtained two EC_{50} values: EC^1_{50} = 2.2 μM and EC^2_{50} = 681 μM. The values were consistent with the values obtained by binding of Rc^{E85Q} to ROS membranes (Fig. 2*B*). The binding at low Ca^{2+} ($^1EC_{50}$ = 2.2 μM) made up 25% of the total binding signal, whereas the binding at high Ca^{2+} contributed to 75% of the total binding signal. Binding at low Ca^{2+} is similar to binding of WT-recoverin to membranes (Figs. 2*B* and 4). Therefore, we interpret the small but significant binding of Rc^{E85Q} to membranes at low Ca^{2+} (EC^1_{50}) as an operative Ca^{2+}-myristoyl switch in the mutant, when only one Ca^{2+} ion is bound to EF-hand 3. Increasing the [Ca^{2+}] led finally to a weak binding of Ca^{2+} to the mutated EF-hand 2 (Figs. 2*B* and 4), which led to a complete exposure of the myristoyl group, but the half-maximal free [Ca^{2+}] at which the exposure took place was shifted to higher [Ca^{2+}].

Kinetics of Dissociation of Myristoylated Forms of WT-Recoverin and Mutant Rc^{E85Q} from Membranes—Sensorgrams recorded with myristoylated forms of WT-recoverin and Rc^{E85Q} exhibited not only different maximal amplitudes but also different dissociation kinetics (Fig. 5). We compared sensorgrams that were recorded at 1 μM and 400 μM Ca^{2+} in the running buffer using myristoylated WT-recoverin and Rc^{E85Q} as analytes. Association of WT-recoverin and Rc^{E85Q} to phospholipids rapidly reached the maximal amplitude. Flushing the flow cell with running buffer, thereby rapidly diluting the recoverin concentration, triggered dissociation of both proteins from immobilized phospholipids. Sensorgrams obtained with Rc^{E85Q} showed a rectangular shape at all tested Ca^{2+} concentrations (see, for example, recordings at 1 μM and 400 μM Ca^{2+} in Fig. 5*A*), which indicates rapid association and dissociation. Corresponding dissociation rate constants were in the order of ≥0.1 s^{-1} (BIAcore Manual, 1993). In comparison, association and dissociation of WT-recoverin at 1 μM free [Ca^{2+}] was also rapid, and recordings of WT-recoverin and Rc^{E85Q} were almost identical (Fig. 5*A*, *bottom*). However, sensorgrams recorded with WT-recoverin became different when the free Ca^{2+} concentration was raised to 400 μM. In particular, the dissociation phase became biphasic and contained a slower component (Fig. 5*A*). Control recordings with protein G and calmodulin showed a much smaller response (Fig. 5*B*), which reflected the rapid change in bulk refractive index.

We analyzed this phenomenon by performing the experiment at different free [Ca^{2+}] within the range of 1 μM to 2 mM using WT-recoverin as analyte. An overlay of corresponding sensorgrams is shown in Fig. 5*C*. To highlight the differences, only the resonance signals at equilibrium and the dissociation phases are displayed in Fig. 5*C*. Increasing free [Ca^{2+}] caused the development of a slower component in the dissociation phase. We were seeking to derive a quantitative description of this effect. First, we tried to fit the data according to a model of two parallel reactions yielding two dissociation rate constants (BIAevaluation software 3.1). By this approach, we obtained a very fast rate constant k_{d1} of ≥0.1 s^{-1} and a slower rate constant of k_{d2} ≤0.01 s^{-1}, corresponding to the fast and slow components of the dissociation phase. Because rapid dissociation rate constants on the order of ≥0.1 s^{-1} cannot be fitted reliably by the BIAevaluation software, we consider these values only a semiquantitative description of the effect. Nevertheless, we conclude that the dissociation of recoverin from the membranes at high free [Ca^{2+}] is slowed by a factor of at least 10, which consequently prolongs the mean residence time of recoverin at membranes.

Then we wanted to know at which free [Ca^{2+}] the development of the slower component was half-maximal. It is evident from visual inspection of the sensorgrams that 10 s after starting the dissociation, the slower component showed a clear Ca^{2+} dependence. Thus, we analyzed the sensorgrams by comparing the relative response at 5, 10, and 20 s after start of the dissociation process (see *arrow* indicating RU_t in Fig. 5*C*). The amplitude of each sensorgram at that time was determined and normalized to the maximal amplitude of the corresponding sensorgram yielding RU_t/RU_{max} (see *arrow* indicating RU_{max} in Fig. 5*C*). These "relative" amplitudes are shown as a function of free [Ca^{2+}] in Fig. 5*D* for a representative set of recordings. Slowing of the dissociation kinetics is manifested as an increase of relative response units RU_t/RU_{max}. The effect was half-maximal at 2–4 μM free [Ca^{2+}] (three sets of recordings),

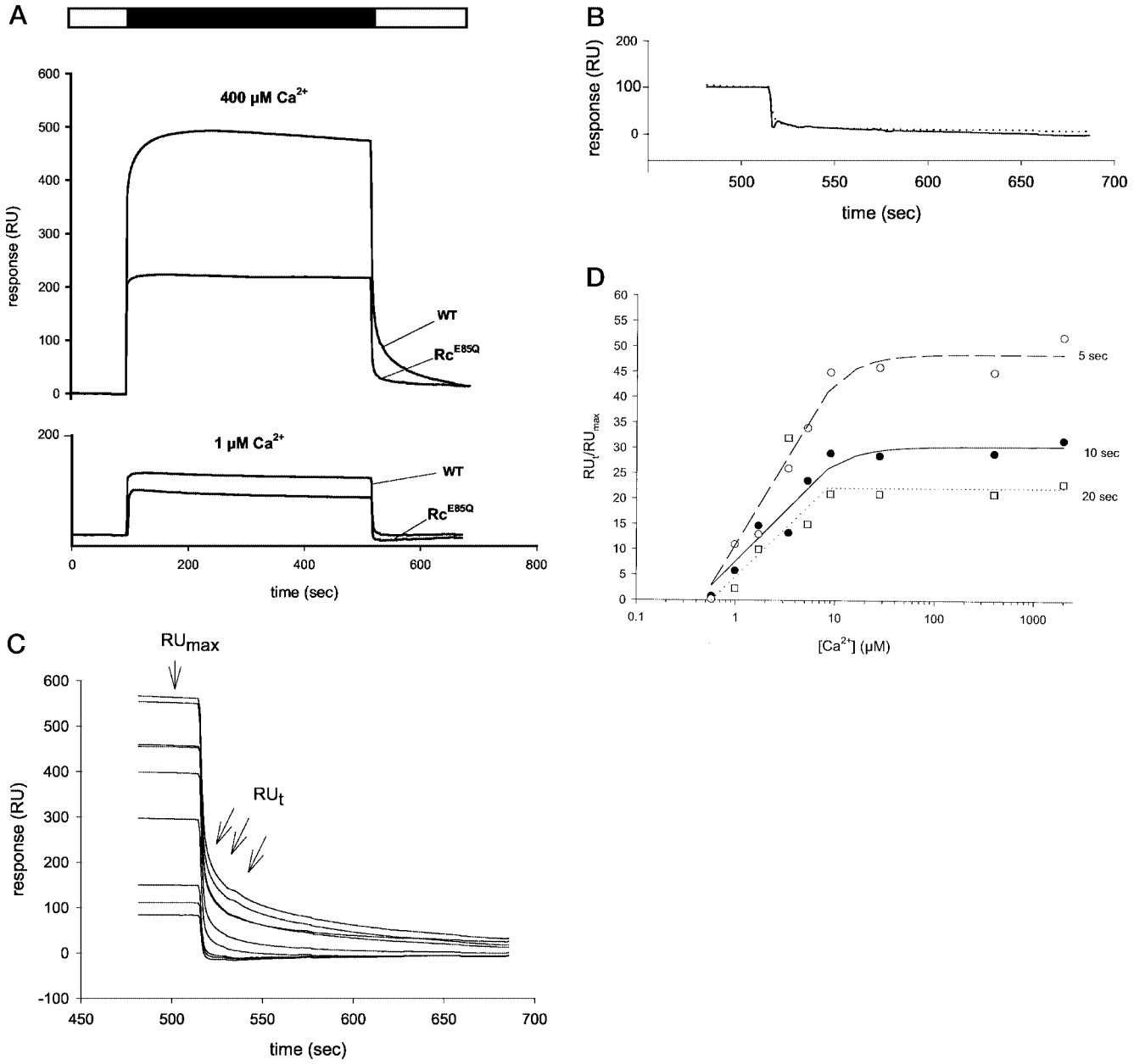

FIG. 5. **Difference in dissociation kinetics of WT-recoverin and Rc^{E85Q}.** *A*, overlay of sensorgrams recorded at 400 μM Ca^{2+} (*top*) and 1 μM Ca^{2+} (*bottom*) with WT-recoverin and Rc^{E85Q} as analyte in the mobile phase (*black bar*). *B*, control recordings with 30 μM calmodulin (dotted line) and protein G (line). *C*, overlay of sensorgrams recorded with 15 μM WT recoverin at different free [Ca^{2+}] (570 nM, 1 μM, 1.7 μM. 3.4 μM, 5.3 μM, 9 μM, 28 μM, 400 μM, and 2 mM). Only a part of the association phase is shown. *Arrows* indicate maximal amplitude, RU_{max}, and the relative amplitudes 5, 10, and 20 s after onset of dissociation (Ru_t). *D*, RU_t/RU_{max} as a function of free [Ca^{2+}] for three different time points. Values of EC_{50} were 2.4 μM $\pm$ 0.9 μM (5 s), 4.1 μM $\pm$ 1.3 μM (10 s), and 4.4 μM $\pm$ 2.3 μM (20 s).

and the Ca^{2+} dependence did not differ much when we analyzed the effect at different time points (Fig. 5*D*; differences in RU_t/RU_{max} at saturation for different time points mirror the decreasing phase of the dissociation signal).

Our data on dissociation of myristoylated WT-recoverin and mutant Rc^{E85Q} from immobilized phospholipids by SPR spectroscopy allow us to conclude that slowing of the dissociation kinetics by increasing free [Ca^{2+}] occurs in WT-recoverin and is conferred by the EF-hand 2.

DISCUSSION

A crystallographic study of myristoylated recoverin has shown that EF-hand 3 has a classic "open conformation" that is also found in prototypical EF-hand proteins such as calmodulin and troponin C (40), whereas the structure of EF-hand 2 differs from these prototypical EF-hand structures. Besides, EF-hand 2 and 3 differ in their affinity for binding Ca^{2+} and might also play different roles in the function of recoverin.

Structural differences between EF-hand 2 and 3 raise the question: which site (or both) must bind Ca^{2+} to expose the myristoyl residue in the myristoyl switch mechanism? NMR studies of WT-recoverin and fluorescence studies of mutants Rc^{E85Q} and Rc^{E121Q} suggest that the binding of Ca^{2+} to recoverin is a sequential process: Ca^{2+} binds first to EF-hand 3 and then to EF-hand 2 (17, 31, 39). Our $^{45}Ca^{2+}$ titration curves (Fig. 1) are in agreement with these findings. If EF-hand 3 is mutated, Ca^{2+} is unable to bind to the native EF-hand 2 (in Rc^{E121Q}), whereas Ca^{2+} can bind to EF-hand 3 when EF-hand 2 is impaired (in Rc^{E85Q}). We hypothesize that myristoylated Rc^{E121Q} is in a locked conformation; because it cannot bind

Ca^{2+} in EF-hand 3, the myristoyl group remains clamped in the hydrophobic cleft and a Ca^{2+}-dependent membrane binding does not occur (Fig. 2).

EF-hand 2 and 3 are located in the two separate domains that form recoverin's compact structure (40). Ames *et al.* (17, 41) proposed that swiveling about glycine at position 96 alters the interaction between EF-hand 2 and EF-hand 3 at the domain interface and thereby induces a structural change in EF-hand 2. This change then increases the affinity for Ca^{2+} in EF-hand 2, which is a necessary step to further trigger the exposure of the myristoyl group. In a recent study, Ames *et al.* showed (30) that the mutant Rc^{E85Q} represents an intermediate state of recoverin along the pathway from the Ca^{2+}-free form (myristoyl group buried) to the fully liganded form (myristoyl group exposed). The myristoyl group is partially unclamped in this intermediate state and has exposed its carbonyl end. We observed that myristoylated Rc^{E85Q} can bind to ROS membranes and immobilized liposomes by a two-step mechanism. A small fraction of Rc^{E85Q} can bind to membranes at low [Ca^{2+}] (2.2–9 μM), whereas the major amount needs millimolar [Ca^{2+}] to fully associate with membranes. The binding of Rc^{E85Q} to membranes at low [Ca^{2+}] probably reflects a new equilibrium state, where the membrane stabilizes an intermediate state with an exposed myristoyl group. The Ca^{2+} binding affinity of the mutated EF-hand 2 is probably shifted in the same way. Thus, we hypothesize the following sequence: in the membrane-free system, the myristoyl group is partially exposed, when one Ca^{2+} is bound, the presence of membranes then leads to a new equilibrium with a higher amount of Rc^{E85Q} that has an exposed myristoyl group.

Our results differ significantly from the work of Matsuda *et al.* (31), who found by the use of a different EF-hand 2 mutant (E85M), that the Ca^{2+} sensitivity of the switch of the E85M mutant is almost identical to that of WT-recoverin. Because our results with mutant Rc^{E85Q} are crucial for the assignment of a specific function to EF-hand 2 (and EF-hand 3), we will discuss possible reasons for these discrepancies. Matsuda *et al.* (31) used a different mutation and a different protein, S-modulin, the frog orthologue of bovine recoverin. So far, S-modulin has exhibited the same biochemical properties as bovine recoverin; therefore, it is unlikely that species differences account for the different observations. Differences in the amino acid substitution at position E85, however, could well lead to different properties of the mutants.

SPR recordings with WT-recoverin and Rc^{E85Q} allowed us further to decipher another property of EF-hand 2. When EF-hand 2 is impaired, recoverin can associate with membranes, but the dissociation from the membranes is very fast both at low and high [Ca^{2+}] (see Fig. 5). This means that there is a rapid equilibrium between the soluble and membrane-bound states of Rc^{E85Q}. WT-recoverin showed a slower dissociation from the membrane when [Ca^{2+}] increased, which would increase the mean residence time of recoverin at the membrane by at least a factor of 10. This effect was half-maximal at 2 to 4 μM [Ca^{2+}] (see Fig. 5, *C* and *D*). Thus, it had Ca^{2+} sensitivity similar to that of the myristoyl switch and was similar to the IC_{50} of rhodopsin kinase inhibition (27, 39–46). EF-hand 2 seems to be critical for the control of rhodopsin kinase activity (31). Alekseev *et al.* (27) found no inhibition of rhodopsin kinase by myristoylated Rc^{E85Q} in the range of 1 to 100 μM Ca^{2+}. However, a small fraction of Rc^{E85Q} (25%) can bind to membranes. How then does the membrane-dependent control of rhodopsin kinase activity work? Is, for example, the increase of time in which recoverin remains associated with membranes at high [Ca^{2+}] important for inhibition of rhodopsin kinase? Work from Satpaev *et al.* (47) indicates that this is a reasonable assumption. These authors measured the apparent k_{on} and k_{off} rates of recoverin and rhodopsin kinase in a membrane-free assay system using SPR spectroscopy. They report an apparent k_{on} of 10^5 $M^{-1}s^{-1}$ and an apparent k_d of 0.1 s^{-1}. The mean residence time of recoverin on the membrane should extend the half-life of the recoverin-rhodopsin kinase complex to allow an effective inhibition. The dissociation rate must therefore be slower than 0.1 s^{-1}, which is the case for WT-recoverin at high [Ca^{2+}] but not for the EF-2 mutant (see Fig. 5).

In summary, by combining our functional experimental data with information on the structure of recoverin (18, 19, 30), we propose the following model of the Ca^{2+}-myristoyl switch of recoverin. In the absence of Ca^{2+} (19) and when EF-hand 3 is mutated (Fig. 2*B*), the myristoyl group is clamped. According to the sequential binding of Ca^{2+} to recoverin (Fig. 1 and Ref. 31), Ca^{2+} binds first to EF-hand 3, which unlocks the clamped myristoyl group and leads to a transition state (30). In this transition state, recoverin has about one quarter of membrane binding activity compared with WT-recoverin. The resulting binding of Ca^{2+} to the second EF-hand increases membrane-binding activity because of the complete exposition of the myristoyl group (18). In addition, we emphasize that EF-hand 2 controls the mean residence time of recoverin at the membrane and that this mechanism is critical for inhibition of rhodopsin kinase by recoverin.

REFERENCES

1. Pitcher, J. A., Freedman, N. J., and Lefkowitz, R. J. (1998) *Annu. Rev. Biochem.* **67,** 653–692
2. Wilden, U., Hall, S. W., and Kühn, H. (1986) *Proc. Natl. Acad. Sci. U. S. A.* **83,** 1174–1178
3. Palczewski, K., and Saari, J. C. (1997) *Curr. Opin. Neurobiol.* **7,** 500–504
4. Dizhoor, A. M., Nekrasova, E. R., and Philippov, P. P. (1991) *Biokhimia* **56,** 225–228
5. Dizhoor, A. M., Ray, S., Kumar, S., Niemi, G., Spencer, M., Brolley, D., Walsh, K. A., Philipov, P. P., Hurley, J. B., and Stryer, L. (1991) *Science* **251,** 915–918
6. Lambrecht, H.-G., and Koch, K.-W. (1991) *EMBO J.* **10,** 793–798
7. Senin, I. I., Koch, K.-W., Akhtar, M., and Philippov, P. P. (2002) *Photoreceptors and Calcium.* Landes Bioscience, Georgetown, TX, in press.
8. Kawamura, S. (1993) *Nature* **362,** 855–857
9. Kawamura, S., Hisatomi, O., Kayada, S., Tokunaga, F., and Kuo, C.-H. (1993) *J. Biol. Chem.* **268,** 14579–14582
10. Pugh, E. N., Jr., Nikonov, S., and Lamb, T. D. (1999) *Curr. Opinion Neurobiol.* **9,** 410–418
11. Pugh, E. N., Jr., and Lamb, T. D. (2000) in *Handbook of Biological Physics.* (Stavenga D. G., DeGrip W. J., and Pugh E. N., Jr., eds) pp 183–255, Elsevier Science B.V., Amsterdam
12. Burns, M. E., and Baylor, D. A. (2001) *Annu. Rev. Neurosci.* **24,** 779–805
13. Fain, G. L., Matthews, H. R., Cornwall, M. C., and Koutalos, Y. (2001) *Physiol. Rev.* **81,** 117–151
14. Zozulya, S., and Stryer, L. (1992) *Proc. Natl. Acad. Sci. U. S. A.* **89,** 11569–11573
15. Dizhoor, A. M., Chen, C.-K., Olshevskaya, E., Sinelnikova, V. V., Phillipov, P., and Hurley, J. B. (1993) *Science* **259,** 829–832
16. Dizhoor, A. M., Ericsson, L. H., Johnson, R. S., Kumar, S., Olshevskaya, E., Zozulya, S., Neubert, T. A., Stryer, L., Hurley, J. B., and Walsh, K. A. (1992) *J. Biol. Chem.* **267,** 16033–16036
17. Ames, J. B., Porumb, T., Tanaka, T., Ikura, M., and Stryer, L. (1995) *J. Biol. Chem.* **270,** 4526–4533
18. Ames, J. B., Ishima, R., Tanaka, T., Gordon, J. I., Stryer, L., and Ikura, M. (1997) *Nature* **389,** 198–202
19. Tanaka, T., Ames, J. B., Harvey, T. S., Stryer, L., and Ikura, M. (1995) *Nature* **376,** 444–447
20. Braunewell, K.-H., and Gundelfinger, E. D. (1999) *Cell Tissue Res.* **295,** 1–12
21. Ames, J. B., Tanaka, T., Stryer, L., and Ikura, M. (1996) *Curr. Opin. Struct. Biol.* **6,** 432–438
22. Burgoyne, R. D., and Weiss, J. L. (2001) *Biochem. J.* **353,** 1–12
23. Godsel, L. M., and Engman, D. M. (1999) *EMBO J.* **18,** 2057–2065
24. Franco, M., Chardin, P., Chabre, M., and Paris, S. (1996) *J. Biol. Chem.* **271,** 1573–1578
25. Goldberg, J. (1998) *Cell* **95,** 237–248
26. McLaughlin, S., and Aderem, A. (1995) *Trends Biochem. Sci.* **20,** 272–276
27. Alekseev, A. M., Shulga-Morskoy, S. V., Zinchenko, D. V., Shulga-Morskaya, S. A., Suchkov, D. V., Vaganova, S. A., Senin, I. I., Zargarov, A. A., Lipkin, V. M., Akhtar, M., and Philippov, P. P. (1998) *FEBS Lett.* **440,** 116–118
28. Strynadka, N. C. J., and James, M. N. G. (1989) *Annu. Rev. Biochem.* **58,** 951–998
29. Moncrief, N. D., Kretsinger, R. H., and Goodman, M. (1990) *J. Mol. Evol.* **30,** 522–562
30. Ames, J. B., Hamasaki, N., and Molchanova, T. (2002) *Biochemistry* **41,** 5776–5787

31. Matsuda, S., Hisatomi, O., and Tokunaga, F. (1999) *Biochemistry* **38,** 1310–1315
32. Koch, K.-W., Lambrecht, H.-G., Haberecht, M., Redburn, D., and Schmidt, H. H. H. W. (1994) *EMBO J.* **13,** 3312–3320
33. Shichi, H., and Somers, R. L. (1978) *J. Biol. Chem.* **253,** 7040–7046
34. Neubert, T. A., Walsh, K. A., Hurley, J. B., and Johnson, R. S. (1997) *Protein Sci.* **6,** 843–850
35. Harrison, S. M., and Bers, D. M. (1987) *Biochim. Biophys. Acta* **925,** 133–143
36. Bradford, M. M. (1976) *Anal. Biochem.* **72,** 248–254
37. Laemmli, U. K. (1970) *Nature* **227,** 680–685
38. Lange, C., and Koch, K.-W. (1997) *Biochemistry* **36,** 12019–12026
39. Permyakov, S. E., Cherskaya, A. M., Senin, I. I., Zargarov, A. A., Shulga-Morskoy, S. V., Alekseev, A. M., Zinchenko, D. V., Lipkin, V. M., Philippov, P. P., Uversky, V. N., and Permyakov, E. A. (2000) *Protein. Eng.* **13,** 783–790
40. Flaherty, K. M., Zozulya, S., Stryer, L., and McKay, D. B. (1993) *Cell* **75,** 709–716
41. Ames, J. B., Ikura, M., and Stryer, L. (2000) *Methods Enzymol.* **316,** 121–132
42. Gorodovikova, E. N., Gimelbrant, A. A., Senin, I. I., and Philippov, P. P. (1994) *FEBS Lett.* **349,** 187–190
43. Gorodovikova, E. N., Senin, I. I., and Philippov, P. P. (1994) *FEBS Lett.* **353,** 171–172
44. Calvert, P. D., Klenchin, V. A., and Bownds, M. D. (1995) *J. Biol. Chem.* **270,** 24127–24129
45. Chen, C.-K., Inglese, J., Lefkowitz, R. J., and Hurley, J. B. (1995) *J. Biol. Chem.* **270,** 18060–18066
46. Klenchin, V. A., Calvert, P. D., and Bownds, M. D. (1995) *J. Biol. Chem.* **270,** 16147–16152
47. Satpaev, D. K., Chen, C.-K., Scotti, A., Simon, M. I., Hurley, J. B., and Slepak, V. Z. (1998) *Biochemistry* **37,** 10256–10262